Nested-ring doping for highly-efficient 1907 nm short wavelength cladding-pumped thulium fiber lasers

MATTHEW J. BARBER[1,*], PETER C. SHARDLOW[1], PRANABESH BARUA[1], JAYANTA K. SAHU[1], AND W. ANDREW CLARKSON[1]

[1] Optoelectronics Research Centre, University of Southampton, University Rd., Southampton, SO17 1BJ, UK
[*] Corresponding author: m.j.barber@soton.ac.uk

Compiled August 21, 2020

Cladding-pumped Tm-doped fiber lasers operating below 1950 nm have difficulty matching the high efficiency, power-scalable output that can be achieved at longer wavelengths. This challenge arises due to the strong three-level behavior at short wavelengths and strong competition from higher-gain long wavelength emission. In this paper, we demonstrate a nested-ring fiber design in which a highly-doped Tm ring is embedded within a larger undoped core. The fiber is specifically tailored for highly efficient and high power short wavelength operation (<1950 nm). The nested-ring Tm fiber laser has generated 62 W of single-mode 1907 nm output with up to 65% (70%) slope efficiency with respect to launched (absorbed) pump power.

http://dx.doi.org/10.1364/ao.XX.XXXXXX

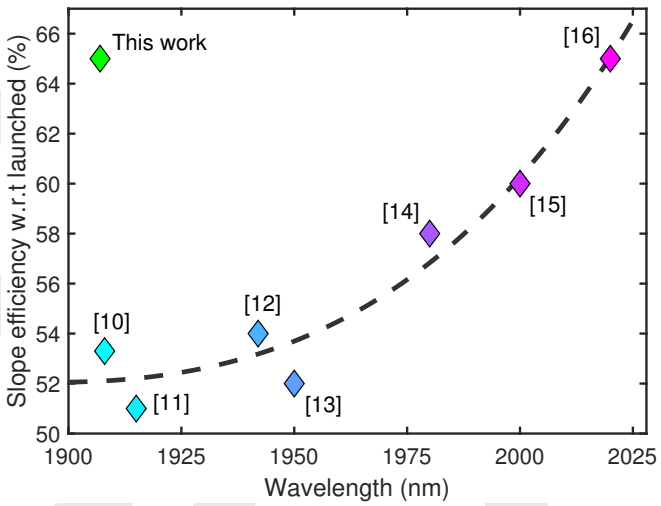

Fig. 1. Reported 790 nm cladding-pumped high power (>50 W) Tm-doped fiber slope efficiencies with respect to launched pump power, as a function of emission wavelength [10–16].

Tm-doped silica fiber lasers provide access to a broad range of emission wavelengths in the near-infrared region from 1660 nm up to 2200 nm [1–3]. Such emission covers an important eye-safe spectral region with applications in plastic materials processing, medical surgery, trace gas sensing, optical communications, LIDAR, optical pumping of laser materials and nonlinear frequency conversion to the mid-infrared band [4–9].

Tm fiber sources operate as quasi-three-level laser systems, demonstrating gain spectra that are dependent on the excitation density in the Tm ions. In order to access the entire range of emission wavelengths, a variety of fiber designs and pumping methods must be utilized to satisfy the different excitation requirements. Reported Tm fiber sources have mainly used 1550 nm core-pumping to target the lower half of the Tm emission spectrum (1660–1900 nm) [1], and 790 nm cladding-pumping for the upper half (1900–2200 nm) [17]. For high power operation, cladding-pumping is preferred due to the ready availability of 790 nm multi-mode pump diodes and the difficulty of power scaling single-mode 1550–1600 nm lasers, which has limited core-pumped Tm sources to <50 W of output power [18]. Furthermore, despite the large quantum defect between 790 nm and 2 µm, Tm fiber lasers benefit from a 'two-for-one' cross-relaxation process [19], that offers the potential for theoretical slope efficiencies exceeding 80% with a sufficiently high Tm concentration. In 790 nm cladding-pumped fibers, the small overlap factor between the pump light and the dopant material produces relatively low Tm excitation densities. This generates a gain spectrum where the longer wavelengths (>1950 nm), which are more four-level in nature, have higher gain than the shorter wavelengths. There can be so much gain available at longer wavelengths that the fiber will begin to emit parasitic lasing at longer wavelengths, irrespective of the wavelength-selective feedback provided. Once parasitic lasing is initiated, the laser gain is clamped and short wavelength operation is unobtainable.

To suppress the parasitic gain at longer wavelengths, gain flattening techniques such as the use of fiberized optical filters or modified material compositions can be implemented, but are challenging to demonstrate over a wide gain bandwidth [20, 21]. Alternatively, the gain for parasitic lasing can be reduced by, for example, shortening the fiber length or lowering the dopant concentration. This decreases the gain preferentially at

longer wavelengths, moving the effective gain peak to shorter wavelengths and favoring short wavelength operation, but at the expense of a reduction in pump absorption efficiency.

A simplified form of the single-pass optical gain in decibels, $G(\lambda)$, for a fiber with a uniformly-doped core can be expressed in terms of the local gain, $g(z,\lambda)$, as:

$$G(\lambda) = 4.343 \int_0^L g(z,\lambda) dz, \quad \textbf{(1)}$$

where

$$g(z,\lambda) = \xi(\lambda) \left[(\sigma_e(\lambda) + \sigma_a(\lambda)) N_2(z) - \sigma_a(\lambda) N_{dop} \right], \quad \textbf{(2)}$$

for which z is the position along the fiber, λ is the wavelength, N_{dop} is the active ion density in the fiber core, $N_2(z)$ is the upper laser manifold population density at position z, $\sigma_e(\lambda)$ is the effective emission cross-section, $\sigma_a(\lambda)$ is the effective absorption cross-section from the lower laser manifold, L is the fiber length and $\xi(\lambda)$ is the spatial overlap factor which describes the fraction of modal power in the active ion doped region [22].

Reduction of the overall gain by shortening the fiber length effectively lowers the number of laser active ions within the gain path, but has the disadvantage of reducing the pump absorption efficiency and hence the overall efficiency. In cladding-pumped fibers, the reduced pump absorption per unit length can be compensated for by fabricating a tighter cladding around the active core. This allows the total number of active ions to be reduced while still maintaining efficient pump absorption. However, the use of a smaller cladding diameter increases the thermal load (due to the laser pumping cycle) per unit length, which limits the power scaling potential of the fiber.

A reduction in the Tm dopant concentration (N_{dop}) can lower the thermal load per unit length again by lengthening the fiber used to achieve a high pump absorption efficiency. However, lowering the Tm dopant concentration will weaken the 'two-for-one' cross-relaxation efficiency, which is most beneficial with a >3.5 wt% doping concentration and is heavily diminished for concentrations below 2 wt% [19]. A dopant reduction of this extent limits the slope efficiency to 50–55%, in contrast to the 65+% that can be attained for highly-doped Tm fibers. As such, for high power cladding-pumped Tm-doped fiber lasers, the slope efficiency with respect to launched pump power drops as the wavelength is decreased because either pump absorption is sacrificed, or a lower Tm dopant concentration fiber is utilized which reduces the cross-relaxation efficiency. This is evident from the reported results shown in Figure 1, which represent the best efficiencies to date for cladding-pumped Tm fiber lasers operating above 50 W.

In this paper, we explore the use of a modified core dopant profile to reduce the overlap factor (ξ) between the propagating core mode and the Tm doped region. The key element of our design, rather than using a uniformly-doped core, is to confine the Tm ions to a thin ring towards the edge of the core thereby reducing the spatial overlap of the propagating LP_{01} mode with the doped region (Figure 2). This dramatically reduces the thermal load per unit length without incurring the penalty of increased gain at longer (parasitic) wavelengths due to the need for a longer fiber for efficient pump absorption. A further attraction of this 'nested-ring' design is that a high Tm doping concentration (>3.5 wt%) can be employed within the ring structure to promote 'two-for-one' cross-relaxation whilst maintaining a low thermal loading density. This permits higher power cladding-pumped Tm lasers with higher efficiency in the wavelength band below 1950 nm. Here, we report on the design, fabrication and all-fiber 1907.3 nm operation of the nested-ring Tm fiber. Pump power limited laser operation up to 62 W of 1907 nm output is achieved for 65% (70%) slope efficiency with respect to launched (absorbed) pump power, with excellent beam quality and no thermal roll-over observed.

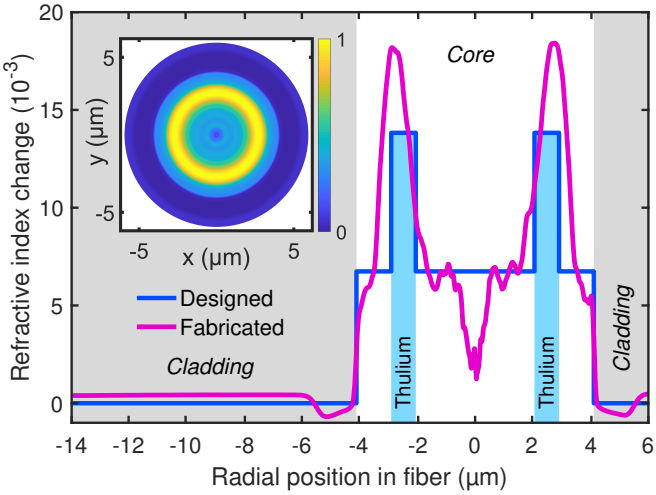

Fig. 2. Refractive index profile of the designed and fabricated nested-ring fiber preform, scaled to an 8.2 μm diameter core. Inset: Normalized 3D map of the nested-ring core geometry.

The Tm-doped nested-ring fiber was designed to be directly compatible with readily-available photosensitive passive fiber commonly used in short wavelength Tm fiber lasers, namely a 10 μm core diameter with 0.15 NA and a 125 μm cladding diameter. The nested-ring fabrication was performed in-house using solution doped modified chemical vapor deposition (MCVD). The preform core was fabricated with two outer germanosilicate layers (target Δn = 0.0067), a solution-doped Tm aluminosilicate layer (≈4 wt% Tm with $\Delta n \approx 0.014$) and a final germanosilicate layer ($\Delta n \approx 0.0067$). The inclusion of Al in the Tm-doped layer reduces the clustering of Tm ions, which can otherwise cause excited state population loss (quenching) in highly-doped fibers. Figure 2 illustrates the preform refractive index profile, scaled down to the target fiber dimensions. The use of high Tm dopant concentrations in the nested-ring raises the refractive index of the doped sections substantially above that of the passive fiber, but by utilizing lower refractive index undoped core layers, the effective NA of the core is reduced.

The refractive index profile of the core dictates the modal content of the propagating signal light. In the nested-ring fiber, the refractive index profile is very similar to the intensity profile of higher-order ring-shaped modes (Figure 2). In order to prevent multi-mode emission, the core diameter is selected to ensure that only the LP_{01} mode is guided. To this end, the nested-ring fiber is designed with a 4 wt% Tm doping concentration and a core diameter of 8.2 μm.

Consideration of the splice loss which may arise due to mode field diameter (MFD) and mode shape mismatches between the active and passive fibers was undertaken during the fiber design. The nested-ring fiber had a calculated MFD of 9 μm at 1907 nm (using Optiwave Optifiber), whilst the passive fiber had an MFD of 10.8 μm at 1907 nm. The propagating mode profile from the core refractive index of the Tm fiber was also simulated. This

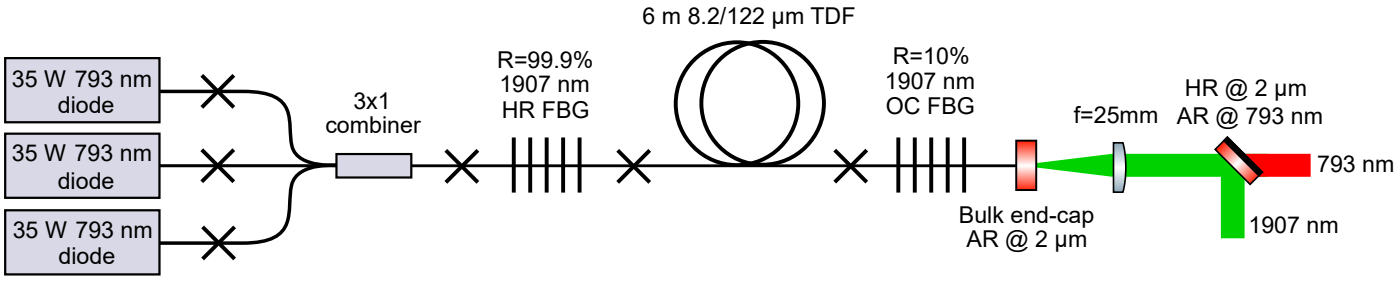

Fig. 3. Tm-doped fiber (TDF) laser setup with 1907 nm high reflectivity (HR) and output coupler (OC) fiber Bragg gratings (FBGs).

showed a slightly super-Gaussian mode profile when compared to the Gaussian mode from a 10 µm 0.15 NA top-hat index step passive fiber. A simple 1D heat diffusion model was used to simulate core diffusion behavior during the formation of a fusion splice between the active and passive fibers. This indicated that the MFD of the nested-ring fiber increases faster than the MFD of the passive fiber, such that we can bring both fibers to the same MFD with the appropriate splice time for low loss transmission.

The preform was overjacketed with an F300 glass tube to match the desired cladding-to-core area ratio, before being shaped to an octagonal geometry with a CO_2 laser to enhance mode scrambling and improve pump absorption [23]. The fiber was drawn to a 122 µm flat-to-flat octagonal cladding diameter (132 µm corner-to-corner diameter) in order to area-match to the 125 µm circular passive fiber. The fiber was drawn with a 180 µm diameter low-index polymer coating (PC-373-AP) to yield 0.46 NA cladding guidance (see inset in Figure 4).

The effective gain of the nested-ring fiber was investigated to predict any changes in the localized gain of the nested-ring fiber when compared to traditional uniform doping. To this end, the fundamental mode profile for the nested-ring core design was simulated using the scaled refractive index profile at a target wavelength of 1907 nm using Optifiber. The overlap integral of the fundamental mode profile and the nested-ring Tm doping profile (ξ) was calculated to be 0.23. As higher-order modes are not guided by the nested-ring structure, only the fundamental mode has been considered in the overlap integral. By comparison, a traditional 10 µm 0.15 NA uniformly-doped fiber has a calculated overlap factor (ξ) of 0.96, implying that the localized gain, $g(z,\lambda)$, is roughly a factor of four lower in the nested-ring fiber over conventional 'top-hat' doping. However, as the nested-ring geometry also extends the fiber length by a factor of four, the length-adjusted localized gain is comparable to that of the uniformly-doped fiber core, but in a much longer fiber length for better thermal management. If instead the dopant material was confined to the center of the core - where the laser mode intensity is greatest - there would only be modest reductions in the overlap factor and the gain, maintaining a low threshold for parasitic lasing at longer wavelengths.

Demonstration of the short wavelength lasing capability of the nested-ring Tm fiber was performed with an all-fiber 1907.3 nm laser as shown in Figure 3. Three 35 W 793 nm diode lasers (DILAS) were combined in a 3×1 pump combiner (Gooch & Housego) to provide 101 W of launched pump power in a 125 µm/0.46 NA fiber. A 6 meter length of nested-ring Tm fiber was spliced to two 1907.3 nm fiber Bragg gratings (FBGs, iXblue), formed of a high reflectivity (HR, R = 99.9%, 1.8 nm bandwidth at -3 dB) and output coupler (OC, R = 10%, 0.5 nm bandwidth at -3 dB) pair. The all-fiber laser configuration (Figure 3) was terminated with an anti-reflection coated bulk end-cap for broadband feedback suppression, with the output light and unabsorbed pump light collimated and separated by a dichroic mirror. The active fiber was wound onto a metal mandrel, encapsulated with UV-curable silicone and mounted on a 15°C water-cooled aluminum plate.

Figure 4 shows the 1907 nm laser output power as a function of launched 793 nm pump power. During operation, 62 W of 1907 nm laser emission is achieved with 93 W of absorbed pump power, limited only by available pump power. The corresponding pump absorption efficiency was 11.4 dB (1.9 dB/m) and in agreement with expectations based on a uniformly-doped fiber, confirming that the core structure has no detrimental impact on pump absorption. The fiber achieved 65% slope efficiency with respect to launched pump power and 70% slope efficiency with respect to absorbed pump power. The theoretical upper limit of slope efficiency with respect to absorbed pump power is ~83% and hence a little higher than our result. We attribute this difference to the variation in Tm concentration across the ring structure, which lowers the overall 'two-for-one' cross-relaxation efficiency. Spectral analysis of the Tm fiber output, shown in Figure 4, confirms 1907 nm emission that is free from parasitic lasing and ASE at 62 W, with a -3 dB emission linewidth of 0.12 nm. Beam quality factor (M^2) measurement yielded M^2 values of 1.03 and 1.00 in orthogonal planes respectively (see Figure 5).

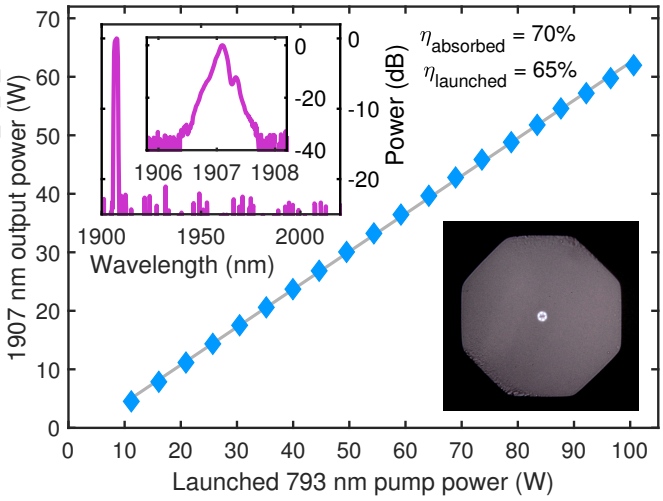

Fig. 4. TDF power curve with 62 W of 1907 nm from 101 W of launched pump with slope efficiency values, η. Inset top-left: emission spectrum at 62 W. Inset bottom-right: cross-sectional view of the fabricated nested-ring fiber.

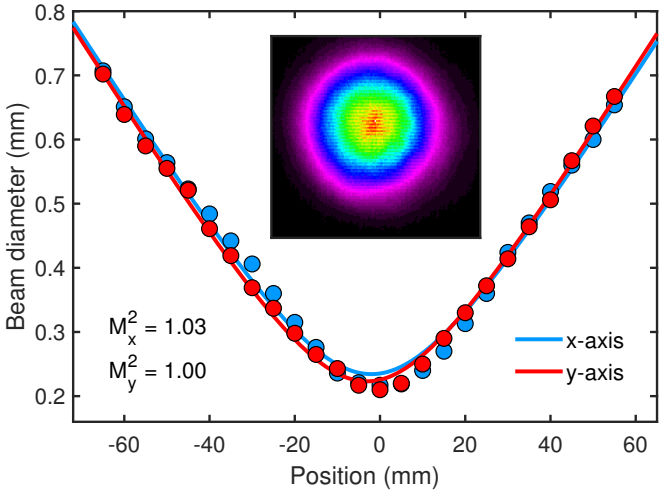

Fig. 5. Beam quality factor (M^2) analysis of the TDF emission at 62 W of 1907 nm. Inset: 1907 nm beam profile at 62 W.

The high slope efficiency of the nested-ring fiber indicates a significant improvement over uniformly-doped 1907 nm Tm fiber lasers. Such performance confirms a high Tm concentration in the doped-ring (with an estimated pump quantum efficiency of 1.68), whilst reducing the pump absorption per unit length by a factor of four to avoid thermally-induced performance reduction.

The challenge of producing high-efficiency cladding-pumped single-mode Tm-doped fiber laser sources emitting at wavelengths shorter than 1950 nm arises from the strong three-level laser character at these wavelengths. To operate here, we must overcome the availability of much higher gain at longer wavelengths, where the laser will naturally operate. Generic gain reduction techniques involve shorter fiber device lengths and lower Tm doping concentrations in the core, which hamper high power and high efficiency operation. Here, we have presented the design and implementation of a nested-ring Tm core structure for improved short-wavelength performance characteristics. Nested layers of Tm-doped and passive glass within the fiber core allow the average Tm dopant of the core to be reduced, whilst maintaining a high localized dopant concentration for enhanced efficiency via 'two-for-one' cross-relaxation. The reduction in the all-wavelength gain of the nested-ring fiber enables the use of device lengths three to four times longer than existing single-mode 1907 nm Tm fiber lasers for considerable power scaling capability without compromising the slope efficiency.

To the best of our knowledge, we report the most efficient single-mode cladding-pumped >50 W Tm fiber laser operating in the sub-1950 nm regime. We have shown pump power limited laser operation capable of generating output powers in excess of 60 W with a slope efficiency of 65% at 1907.3 nm with respect to launched pump power. The laser efficiency improvements highlight the potential benefits of a structured core dopant profile for short wavelength emission, exceeding the capabilities achieved in traditional uniformly-doped Tm fiber lasers. The absence of thermal roll-over in the laser power curve suggests that the nested-ring fiber design will readily allow further power scaling. An estimate of the thermal damage limit for the outer-coating suggests that >300 W pump power can be launched before the onset of damage.

ACKNOWLEDGMENTS

This work was supported by funding from the Defence Science and Technology Laboratory (Dstl, UK) and the Defence Science and Technology group (DST, Australia). M.J.B. acknowledges financial support from the Engineering and Physical Sciences Research Council (EPSRC, UK) and Leonardo, UK. The figure data can be found at https://doi.org/10.5258/SOTON/D1443.

DISCLOSURES

The authors declare no conflicts of interest.

REFERENCES

1. J. M. O. Daniel, N. Simakov, M. Tokurakawa, M. Ibsen, and W. A. Clarkson, Opt. Express **23**, 18269 (2015).
2. T. S. McComb, R. A. Sims, C. C. C. Willis, P. Kadwani, V. Sudesh, L. Shah, and M. Richardson, Appl. Opt. **49**, 6236 (2010).
3. J. Li, Z. Sun, H. Luo, Z. Yan, K. Zhou, Y. Liu, and L. Zhang, Opt. Express **22**, 5387 (2014).
4. I. Mingareev, F. Weirauch, A. Olowinsky, L. Shah, P. Kadwani, and M. Richardson, Opt. Laser Technol. **44**, 2095 (2012).
5. N. M. Fried, Lasers Surg. Medicine **37**, 53 (2005).
6. T. Yin, Y. Song, X. Jiang, F. Chen, and S. He, Opt. Express **27**, 15794 (2019).
7. Z. Li, A. M. Heidt, J. M. O. Daniel, Y. Jung, S. U. Alam, and D. J. Richardson, Opt. Express **21**, 9289 (2013).
8. J. Y. Beyon, Opt. Eng. **46**, 116201 (2007).
9. A. Hemming, J. Richards, A. Davidson, N. Carmody, S. Bennetts, N. Simakov, and J. Haub, Opt. Express **21**, 10062 (2013).
10. B. R. Johnson, D. Creeden, J. Limongelli, H. Pretorius, J. Blanchard, and S. D. Setzler, "Comparison of high power large mode area and single mode 1908nm Tm-doped fiber lasers," in *SPIE Proceedings Volume 9728, Fiber Lasers XIII,* J. Ballato, ed. (2016), p. 972810.
11. Y.-B. Xing, L. Liao, F. Bu, Y.-B. Wang, J.-G. Peng, N.-L. Dai, and J.-Y. Li, Chin. Phys. Lett. **32**, 034204 (2015).
12. Y. Wang, J. Yang, C. Huang, Y. Luo, S. Wang, Y. Tang, and J. Xu, Opt. Express **23**, 2991 (2015).
13. N. Simakov, A. V. Hemming, A. Carter, K. Farley, A. Davidson, N. Carmody, M. Hughes, J. M. O. Daniel, L. Corena, D. Stepanov, and J. Haub, Opt. Express **23**, 3126 (2015).
14. J. Liu, H. Shi, C. Liu, and P. Wang, "Widely-tunable High-power Narrow-linewidth Thulium-doped all-fiber Superfluorescent Source," in *CLEO: 2015,* (OSA, Washington, D.C., 2015), p. JTh2A.98.
15. Jiang Liu, Kun Liu, Fangzhou Tan, and Pu Wang, IEEE J. Sel. Top. Quantum Electron. **20**, 497 (2014).
16. P. C. Shardlow, D. Jain, R. Parker, J. Sahu, and W. A. Clarkson, "Optimising Tm-Doped Silica Fibres for High Lasing Efficiency," in *European Conference on Lasers and Electro-Optics,* (2015), pp. CJ–14–3.
17. A. Sincore, J. D. Bradford, J. Cook, L. Shah, and M. C. Richardson, IEEE J. Sel. Top. Quantum Electron. **24**, 1 (2018).
18. M. D. Burns, P. C. Shardlow, P. Barua, T. L. Jefferson-Brain, J. K. Sahu, and W. A. Clarkson, Opt. Lett. **44**, 5230 (2019).
19. S. D. Jackson and S. Mossman, Appl. Opt. **42**, 2702 (2003).
20. M. Yamada, T. Kanamori, Y. Terunuma, K. Oikawa, M. Shimizu, S. Sudo, and K. Sagawa, IEEE Photonics Technol. Lett. **8**, 882 (1996).
21. P. Wysocki, J. Judkins, R. Espindola, M. Andrejco, and A. Vengsarkar, IEEE Photonics Technol. Lett. **9**, 1343 (1997).
22. S. Jackson and T. King, J. Light. Technol. **17**, 948 (1999).
23. P. C. Shardlow, R. Standish, J. Sahu, and W. Clarkson, "Cladding Shaping of Optical Fibre Preforms via CO2 Laser Machining," in *European Conference on Lasers and Electro-Optics,* (2015), pp. CJ–P.